Scientific Research Publishing

Open Journal of Composite Materials, 2022, 12, 41-55
https://www.scirp.org/journal/ojcm
ISSN Online: 2164-5655
ISSN Print: 2164-5612

Wettability Control between Oleophobic/Superhydrophilic and Superoleophilic/Superhydrophobic Characteristics on the Modified Surface Treated with Fluoroalkyl End-Capped Oligomers/Micro-Sized Polystyrene Particle Composites

Hideo Sawada*, Koki Arakawa, Yuta Aomi

Department of Frontier Materials Chemistry, Graduate School of Science and Technology, Hirosaki University, Hirosaki, Japan
Email: *hideosaw@hirosaki-u.ac.jp

How to cite this paper: Sawada, H., Arakawa, K. and Aomi, Y. (2022) Wettability Control between Oleophobic/Superhydrophilic and Superoleophilic/Superhydrophobic Characteristics on the Modified Surface Treated with Fluoroalkyl End-Capped Oligomers/Micro-Sized Polystyrene Particle Composites. *Open Journal of Composite Materials*, **12**, 41-55.
https://doi.org/10.4236/ojcm.2022.121004

Received: October 27, 2021
Accepted: January 17, 2022
Published: January 20, 2022

Abstract

Fluoroalkyl end-capped vinyltrimethoxysilane-*N*,*N*-dimethylacrylamide cooligomer [R_F-(CH_2-CHSi(OMe)$_3$)$_x$-(CH_2-CHC(=O)NMe_2)$_y$-R_F; R_F = $CF(CF_3)OC_3F_7$: R_F-(VM)$_x$-(DMAA)$_y$-R_F] was synthesized by reaction of fluoroalkanoyl peroxide [R_F-C(=O)O-O(O=)C-R_F] with vinyltrimethoxysilane (VM) and *N*,*N*-dimethylacrylamide (DMAA). The modified glass surface treated with the cooligomeric nanoparticles [R_F-(VM-$SiO_{3/2}$)$_x$-(DMAA)$_y$-R_F] prepared under the sol-gel reaction of the cooligomer under alkaline conditions was found to exhibit an oleophobic/superhydrophilic property, although the corresponding fluorinated homooligomeric nanoparticles [R_F-(VM-$SiO_{3/2}$)$_n$-R_F] afforded an oleophobic/hydrophobic property on the modified surface under similar conditions. R_F-(VM-$SiO_{3/2}$)$_n$-R_F/R_F-(VM-$SiO_{3/2}$)$_x$-(DMAA)$_y$-R_F/***PSt*** (micro-sized polystyrene particles) composites, which were prepared by the sol-gel reactions of the corresponding homooligomer and cooligomer in the presence of ***PSt*** particle under alkaline conditions, provided an oleophobic/superhydrophilic property on the modified surface. However, it was demonstrated that the surface wettability on the modified surface treated with the R_F-(VM-$SiO_{3/2}$)$_n$-R_F/R_F-(VM-$SiO_{3/2}$)$_x$-(DMAA)$_y$-R_F/***PSt*** composites changes dramatically from oleophobic/superhydrophilic to superoleophilic/superhydrophilic and superoleophilic/superhydrophobic characteristics, increasing with greater feed ratios (mg/mg) of the R_F-(VM)$_n$-R_F homooligomer in homooligomer/cooligomer from

0 to 100 in the preparation of the composites. Such controlled surface wettability was also studied by FE-SEM-EDX analyses.

Keywords

Fluorinated Oligomeric Composite, Micro-Sized Polystyrene Particle, Surface Modification, Surface Wettability Change, Oleophobic/Superhydrophilic Property, Superoleophilic/Superhydrophobic Property

1. Introduction

Considerable interest has been hitherto focused on micro-sized inorganic and organic particles, such as silica gel [1]-[6], the ion-exchange resin (cationic or anionic cross-linked polymer beads) [7] [8] [9] [10], and titanium oxide [11] [12] [13], because these particles have a wide range of practical use such as adsorbents for metal ions and white pigments in the plastic industry [1]-[13]. Therefore, from the additional applicable viewpoint of these particles, it is of particular importance to develop new micro-sized particles possessing unique wettability such as oleophobic/superhydrophilic or superolophilic/superhydrophobic characteristics on their surfaces. The modified silica nanoparticles possessing superhydrophobic property on the surface can be easily prepared by the sol-gel reaction of the silica nanoparticles with octadecyltrichlorosilane [14] [15]; however, studies on the preparation and application of fluoroalkylated microsize-controlled particles possessing unique surface wettability such as superoleophilic/superhydrophobic characteristics imparted by fluorine have been very limited except for our recent reports, so far [16] [17]. In fact, we have recently found that fluoroalkyl end-capped vinyltrimethoxysilane oligomer [R_F-$(CH_2CHSi(OMe)_3)_n$-R_F; R_F = $CF(CF_3)OC_3F_7$: R_F-$(VM)_n$-R_F] can be applied to the preparation of the corresponding oligomer/micro-sized silica particle composites possessing the superoleophilic/superhydrophobic property on the composite particle surface, affording a selective removal ability of fluorinated aromatic compounds from aqueous solutions [17]. On the other hand, we previously reported that two fluoroalkyl end-capped vinyltrimethoxysilane—acryloylmorpholine cooligomer can reveal the oleophobic/superhydrophilic property on the glass surface through the flip-flop motion between the fluoroalkyl groups and hydrophilic morpholino units in cooligomer on the modified surface under the environmental change from air to water [18]. From this point of view, it is of particular interest to explore novel fluoroalkyl end-capped oligomers/micro-sized particle composites possessing unique wettability on their surface. Here we report that fluoroalkyl end-capped vinyltrimethoxysilane homooligomer/fluoroalkyl end-capped vinyltrimethoxysilane-*N*,*N*-dimethylacrylamide cooligomer/micro-sized polystyrene particle (***PSt***) composites, which are prepared by the sol-gel reactions of the corresponding homooligomer and cooligomer in the presence of ***PSt*** particle under alkaline conditions, can exhibit the wettability-controlled behavior from highly oleophobic/superhy-

drophilic to superoleophilic/superhydrophobic characteristics on their surfaces, increasing with greater feed ratios of the homooligomer in homooligommer/cooligomer in the preparation of the composites.

2. Experimental

2.1. Measurements

Micrometer size-controlled composite particles were analyzed by using laser diffraction particle size analyzer: Shimadzu SALD-200 V (Kyoto, Japan). Molecular weights of R_F-$(VM)_n$-R_F homooligomer and R_F-$(VM)_x$-$(DMAA)_y$-R_F cooligomer were measured by using a Shodex DS-4 (pump, Tokyo, Japan) and Shodex RI-71 (detector) gel permeation chromatography calibrated with polystyrene standard using teterahydrofuran as the eluent. The contact angles were measured by the use of Kyowa Interface Science Drop Master 300 (Saitama, Japan). Field emission scanning electron micrograph (FE-SEM) was recorded by using JEOL JSM-7000F (Tokyo, Japan). Energy dispersive X-ray (EDX) spectra were obtained using JEOL JSM-7000F (Tokyo, Japan). NMR spectra were measured using a JEOL JNM-400 (400 MHz).

2.2. Materials

Vinyltrimethoxysilane was used as received from Dow Corning Toray Co., Ltd. (Tokyo, Japan). Aqueous ammonia was purchased from FUJIFILM Wako Pure Chemical Industries (Osaka, Japan). *N*,*N*-dimethylacrylamide and micro-sized (cross-linked) polystyrene particles (average particle size: 102 m) were received from Kj Chemicals Corporation (Tokyo, Japan) and Tokyo Chemical Ind., Co., Ltd. (Tokyo, Japan), respectively. Fluoroalkyl end-capped vinyltrimethoxysilane homooligomer [R_F-$(CH_2$-$CHSi(OMe)_3)_n$-R_F: the mixture of dimer and trimer; R_F = $CF(CF_3)OC_3F_7$ (R_F-$(VM)_n$-R_F); Mn = 780] was synthesized by reaction of fluoroalkanoyl peroxide with the corresponding monomer according to our previously reported method [19]. Fluoroalkyl end-capped vinyltrimethoxysilane—*N*,*N*-dimethylacrylamide cooligomer [R_F-$(CH_2$-$CHSi(OMe)_3)_x$-$(CH_2CH(C{=}O)NMe_2)_y$-R_F; R_F = $CF(CF_3)OC_3F_7$ [R_F-$(VM)_x$-$(DMAA)_y$-R_F]; Mn = 2300, x:y = 3:97 (cooligomerization ratio (*x*:*y*) was determined by ^{1}H NMR)] was synthesized based on our previously reported method [18]. Glass plate (borosilicate glass) [micro cover glass: 18 mm × 18 mm] was purchased from Matsunami glass Ind., Ltd. (Osaka, Japan) and was used after washing well with dichloromethane.

2.3. Preparation of Fluoroalkyl End-Capped Vinyltrimethoxysilane Homooligomer/Fluoroalkyl End-Capped Vinyltrimethoxysilane–*N*,*N*-Dimethylacrylamide Cooligomer/Micro-Sized Polystyrene Composites [R_F-$(VM\text{-}SiO_{3/2})_n$-R_F/R_F-$(VM\text{-}SiO_{3/2})_x$-$(DMAA)_y$-R_F/*PSt*]

A typical procedure for the preparation of R_F-$(VM\text{-}SiO_{3/2})_n$-R_F/R_F-$(VM\text{-}SiO_{3/2})_x$-$(DMAA)_y$-R_F/***PSt*** composites is as follows: To methanol solution (5 ml) contain-

ing R_F-$(VM)_n$-R_F homooligomer (70 mg) and R_F-$(VM)_x$-$(DMAA)_y$-R_F cooligomer (30 mg) was added ***PSt*** particle (200 mg). The mixture was stirred with a magnetic stirring bar at room temperature for 10 min. 25% aqueous ammonia solution (2.0 ml) was added to the methanol solution, and was successively stirred at room temperature for 5 h. After the solvent was evaporated off, methanol was added to the obtained crude products. The methanol suspension thus obtained was stirred with magnetic stirring bar at room temperature for 1 day, and then was centrifuged for 30 min. The expected R_F-$(VM\text{-}SiO_{3/2})_n$-R_F/R_F-$(VM\text{-}SiO_{3/2})_x$-$(DMAA)_y$-R_F/***PSt*** composites were easily separated from the methanol solution, and were successively washed several times with methanol. After centrifugal separation of this solution, the obtained product was dried under vacuum at 50˚C for 1 day to produce the purified composites as the white-colored powders (150 mg). Other composites were prepared under similar conditions. The results are shown in Table 1.

2.4. Preparation of Modified Glass Treated with the R_F-$(VM\text{-}SiO_{3/2})_n$-R_F/R_F-$(VM\text{-}SiO_{3/2})_x$-$(DMAA)_y$-R_F/*PSt* Composites

To methanol solution (5 ml) containing R_F-$(VM)_n$-R_F homooligomer (70 mg) and R_F-$(VM)_x$-$(DMAA)_y$-R_F cooligomer (30 mg) was added ***PSt*** particle (200 mg). The mixture was stirred with a magnetic stirring bar at room temperature for 10 min. 25% aqueous ammonia solution (2.0 ml) was added to the methanol solution, and was successively stirred at room temperature for 5 hrs. The glass plate was dipped into this methanol solution at room temperature and left for 1 min. This plate was lifted from the solutions at a constant rate of 0.5 mm/min and subjected to the treatment for 1 day at room temperature; finally, this modified glass plate was dried under vacuum for 1 day at room temperature. After drying, the contact angles of dodecane and water were measured by the deposit of each droplet (2 μl) on the modified glass at room temperature.

3. Results and Discussion

R_F-$(VM)_n$-R_F homooligomer and R_F-$(VM)_x$-$(DMAA)_y$-R_F cooligomer were found to suffer the sol-gel reaction in the presence of micro-sized polystyrene particle (***PSt***) in methanol under alkaline conditions, providing the expected R_F-$(VM\text{-}SiO_{3/2})_n$-R_F/R_F-$(VM\text{-}SiO_{3/2})_x$-$(DMAA)_y$-R_F/***PSt*** composites in 36% - 70% isolated yields as shown in Scheme 1 and Table 1.

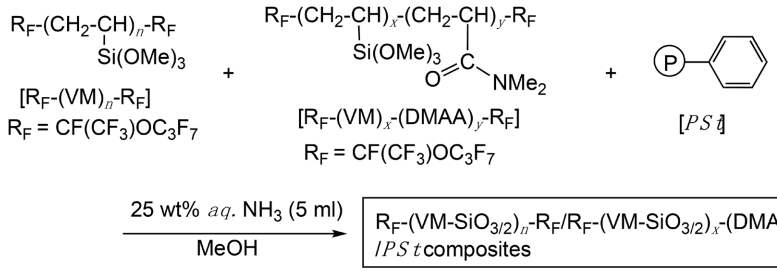

Scheme 1. Preparation of R_F-$(VM\text{-}SiO_{3/2})_n$-R_F/R_F-$(VM\text{-}SiO_{3/2})_x$-$(DMAA)_y$-R_F/***PSt*** composites.

Table 1. Preparation of R_F-(VM-$SiO_{3/2}$)$_n$-R_F/R_F-(VM-$SiO_{3/2}$)$_x$-(DMAA)$_y$-R_F/***PSt*** composites.

Run	Feed ratio[a] (mg/mg/mg)	Yield[b] (%)	Particle size of the composites[c] (μm)
original ***PSt***			101.7 ± 0.07
1	0/100/200	41	104.0 ± 0.07
2	10/90/200	47	124.9 ± 0.07
3	20/80/200	52	118.2 ± 0.11
4	30/70/200	51	119.6 ± 0.14
5	60/40/200	48	119.2 ± 0.07
6	70/30/200	50	125.0 ± 0.10
7	72/28/200	70	121.1 ± 0.07
8	74/26/200	62	126.3 ± 0.07
9	76/24/200	67	116.5 ± 0.07
10	90/10/200	36	120.6 ± 0.07
11	100/0/200	59	124.7 ± 0.06

[a]R_F-(VM)$_n$-R_F/R_F-(VM)$_x$-(DMAA)$_y$-R_F/***PSt***; [b]Yield is based on R_F-(VM)$_n$-R_F, R_F-(VM)$_x$-(DMAA)$_y$-R_F and ***PSt***; [c]Determined by Laser diffraction particle size distribution measurement in methanol.

It was demonstrated that each obtained composite in Table 1 can give a good dispersibility toward methanol. Thus, we have measured the average particle size of these composites in methanol by laser diffraction analysis measurements at room temperature, and the results are also shown in Table 1.

As shown in Table 1, each size of the composites is micrometer size-controlled from 104 to 126 μm. We can observe the increase of the size of the obtained composites, compared to that (102 μm) of the original ***PSt*** particle, indicating that the composite reaction with fluorinated homo- and cooligomers illustrated in Scheme 1 should proceed smoothly to give the expected fluorinated oligomeric ***PSt*** composites. FE-SEM (Field Emission Scanning Electron Microscopy) photographs and EDX (Energy dispersive X-ray) mapping micrographs of the fluorinated composites (Run 6 in Table 1) have been recorded in order to clarify the formation of the R_F-(VM-$SiO_{3/2}$)$_n$-R_F/R_F-(VM-$SiO_{3/2}$)$_x$-(DMAA)$_y$-R_F/***PSt*** composites. FE-SEM photographs and EDX mapping micrographs of the pristine ***PSt*** particle were also measured under similar conditions, for comparison. These results are shown in Figure 1.

Figure 1 reveals that the R_F-(VM-$SiO_{3/2}$)$_n$-R_F/R_F-(VM-$SiO_{3/2}$)$_x$-(DMAA)$_y$-R_F/***PSt*** composites consist of the micro-sized ***PSt*** particles and the R_F-(VM-$SiO_{3/2}$)$_n$-R_F homooligomeric and the R_F-(VM-$SiO_{3/2}$)$_x$-(DMAA)$_y$-R_F cooligomeric nanoparticles. In fact, R_F-(VM)$_n$-R_F homooligomer [R_F = $CF(CF_3)OC_3F_7$] can provide the corresponding homooligomeric nanoparticles with a mean diameter of 72 nm through the similar sol-gel reaction illustrated in Scheme 1 (see Figure 2(A)).

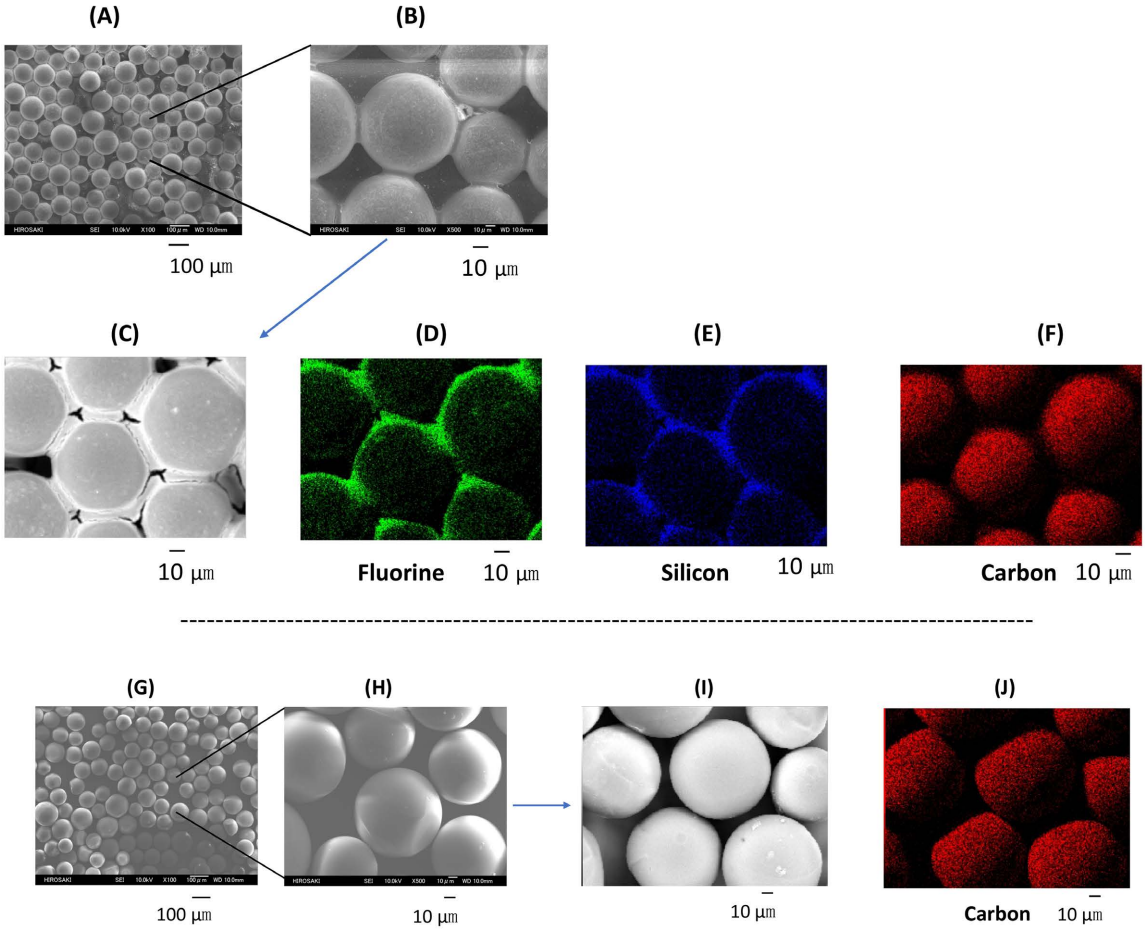

Figure 1. FE-SEM (Field Emission Scanning Electron Micrograph) images of the R_F-(VM-$SiO_{3/2}$)$_n$-R_F/R_F-(VM-$SiO_{3/2}$)$_x$-(DMAA)$_y$-R_F/***PSt*** composites ((A) and (B): Run 6 in **Table 1**) and the pristine ***PSt*** particle (G) and (H), and EDX (Energy Dispersive X-ray) mapping micrographs of fluorine (D), silicon (E), and carbon (F) atoms of the composites ((C): Run 6 in **Table 1**), and carbon (J) atom of the pristine ***PSt*** particle (I)).

We have also succeeded in preparing the R_F-(VM-$SiO_{3/2}$)$_x$-(DMAA)$_y$-R_F cooligomeric nanoparticles [R_F = $CF(CF_3)OC_3F_7$] with a mean diameter of 47 nm by the use of the corresponding cooligomer according to the similar sol-gel reaction to that of **Scheme 1** (see **Figure 2(B)**). Especially, EDX mapping micrographs (**Figures 1(C)-(F)**) on the R_F-(VM-$SiO_{3/2}$)$_n$-R_F/R_F-(VM-$SiO_{3/2}$)$_x$-(DMAA)$_y$-R_F/*PSt* composites and original ***PSt*** particles (**Figure 1(I)** and **Figure 1(J)**) show that fluorine (green-colored area) and silicon (blue-colored are) related to the fluorinated homo- and co-oligomer in the composites are uniformly dispersed between the ***PSt*** particles (red-colored area), in addition to the ***Pst*** particles surface.

Next, we tried to study on the surface wettability of the R_F-(VM-$SiO_{3/2}$)$_n$-R_F/R_F-(VM-$SiO_{3/2}$)$_x$-(DMAA)$_y$-R_F/***PSt*** composites depicted in **Table 1** through the dodecane and water contact angle measurements at room temperature. The results are shown in **Table 2**.

As shown in **Table 2**, it was clarified that the surface wettability of the composites is dependent upon the feed ratio of the homooligomer and the cooligomer

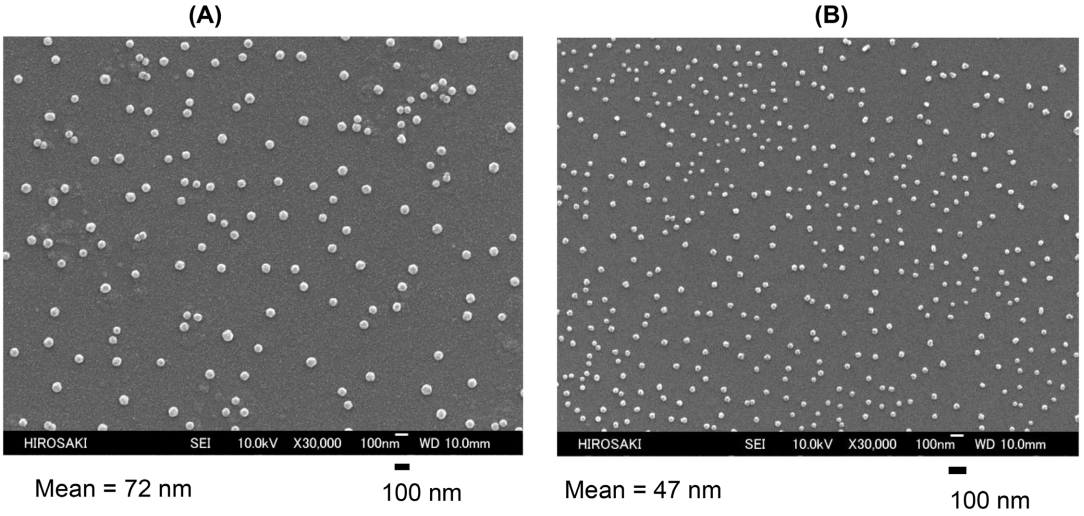

Figure 2. FE-SEM (Field Emission Scanning Electron Micrograph) images of the R_F-(VM-$SiO_{3/2}$)$_n$-R_F homooligommeric nanoparticles (A) and the R_F-(VM-$SiO_{3/2}$)$_x$-(DMAA)$_y$-R_F cooligomeric nanoparticles (B).

Table 2. Contact angles of dodecane and water on the modified glass surface treated with the R_F-(VM-$SiO_{3/2}$)$_n$-R_F/R_F-(VM-$SiO_{3/2}$)$_n$-(DMAA)$_m$-R_F/***PSt*** composites, R_F-(VM-$SiO_{3/2}$)$_n$-R_F homooligomeric nanoparticles, and the R_F-(VM-$SiO_{3/2}$)$_x$-(DMAA)$_y$-R_F cooligomeric nanoparticles.

Run[a]	Feed ratio[b] (mg/mg/mg)	Contact angle (degree) Dodecane	Water
1	0/100/200	69	0
2	10/90/200	70	0
3	20/80/200	70	0
4	30/70/200	74	0
5	60/40/200	82	0
6	70/30/200	88	0
7	72/28/200	68	0
8	74/26/200	35	0
9	76/24/200	0	0
10	90/10/200	0	0
11	100/0/200	0	180
R_F-(VM-$SiO_{3/2}$)$_n$-R_F homooligomeric nanoparticles		59	107
R_F-(VM-$SiO_{3/2}$)$_x$-(DMAA)$_y$-R_F cooligomeric nanoparticles		60	0

[a]Each Run No. corresponds to that of Table 1; [b]R_F-(VM)$_n$-R_F/R_F-(VM)$_x$-(DMAA)$_y$-R_F/***PSt***.

employed for the preparation of the composites, and the higher feed ratios of homooligomer from 0 (Run 1) to 70 mg (Run 6) supply the higher oleophobic characteristic, because the dodecane contact angle value was found to increase from 69 to 88 degrees. However, the additional higher feed ratios of homooligomer from 72 (Run 7) to100 mg (Run 11) afforded the decrease of the dode-

cane contact angle values from 68 to 0 degrees to provide a superoleophilic property on the composite surface. In contrast, we can keep the same water contact angle value: 0 degree in each composite except for Run 11. That is, the R_F-(VM-$SiO_{3/2})_x$-$(DMAA)_y$-R_F/***PSt*** composites (Run 11) were found to give a superoleophilic/superhydrophobic characteristic (dodecane and water contact angle values are 0 and 180 degrees, respectively) on the composite surface. In this case, water contact angle value: 180 degrees (superhydrophobic characteristic) indicate that we cannot deposit water droplets on the modified surface.

The modified surfaces treated with the R_F-$(VM\text{-}SiO_{3/2})_n$-R_F homooligomeric nanoparticles and the R_F-$(VM\text{-}SiO_{3/2})_x$-$(DMAA)_y$-R_F cooligomeric nanoparticles can reveal the oleophobic/hydrophobic and oleophobic/superhydrophilic properties, because dodecane and water contact angle values are 59 and 107 degrees, and 60 and 0 degrees, respectively (see Table 2). Such unique surface wettability would be due to the solubility of the pristine homooligomer and cooligomer. Because, R_F-$(VM)_n$-R_F homooligomer can give a good solubility toward traditional organic media such as methanol, 2-propanaol, chloroform, 1,2-dichloroethane, tetrahydrofuran, dimethyl sulfoxide, *N*,*N*-dimethylformamide and fluorinated aliphatic solvents [1:1 mixed solvents (AK-225^{TR}) of 1, 1-dichloro-2, 2, 3, 3, 3-pentafluoropropane and 1, 3-dichloro-1, 2, 2, 3, 3-pentafluoropropane] except for water; however, R_F-$(VM)_x$-$(DMAA)_y$-R_F cooligomer were found to provide a good solubility for not only these common organic media but also water. Thus, the higher affinity toward water to give the superhydrophilic property toward the composites is due to the presence of the hydrophilic DMAA units in the cooligomer. As mentioned before, the oleophobic/superhydrophilic property related to the cooligomeric nanoparticles is due to the flip-flop motion between the fluoroalkyl groups and hydrophilic DMAA units on the nanoparticle surface under the environmental change from air to water [17]. In this way, superhydrophilic characteristic derived from the composites (Run 1 ~ Run 10) would be due to the presence of the hydrophilic DMAA units in the composites. Therefore, we cannot observe the superhydrophilic or hydrophilic characteristic in the case of the R_F-$(VM\text{-}SiO_{3/2})_n$-R_F/***PSt*** composites possessing no hydrophilic DMAA units in the composites (see Run 11 in Table 2).

In order to clarify such unique surface wettability change related to the present fluorinated composites, EDX mapping micrographs of some fluorinated composites in Table 1 have been measured, and the results are shown in Figure 3 including the original ***PSt*** particle (Figure 1(I)).

Figure 3 reveals that the fluorinated cooligommer in the R_F-$(VM\text{-}SiO_{3/2})_n$-R_F/R_F-$(VM\text{-}SiO_{3/2})_x$-$(DMAA)_y$-R_F/***PSt*** composites is likely to be arranged on the orifice between the ***PSt*** particles, in addition to the ***PSt*** particle surface in the cases of the feed ratios of the cooligomer from 100 to 30 mg as indicated in Runs 1, 5 and 6, providing the oleophobic (dodecane contact angle values: 69, 82 and 88 degrees)/superhydrophilic characteristic (each water contact angle value: 0 degree) (see also Table 2). Decrease of the feed ratios of the cooligomer from

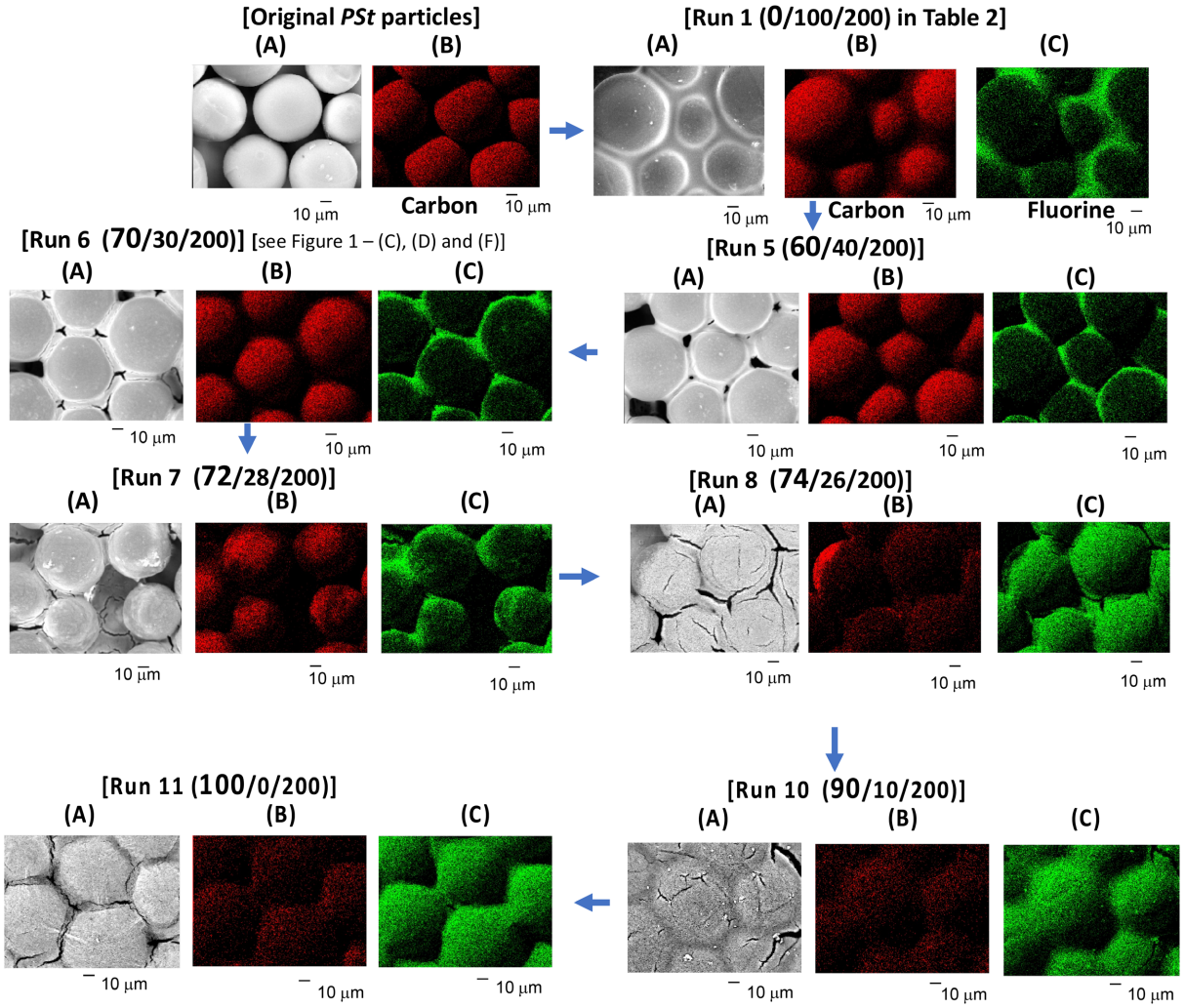

Figure 3. EDX mapping micrographs of carbon (B) and fluorine (C) atoms of the R_F-(VM-$SiO_{3/2}$)$_n$-R_F/R_F-(VM-$SiO_{3/2}$)$_x$-(DMAA)$_y$-R_F/***PSt*** composites ((A): Runs 1, 5, 6, 7, 8, 10 and 11 in Table 1) and the pristine ***PSt*** particle (A)).

100 to 30 mg, that is, the higher feed ratios of the homooligomer from 0 to 70 mg can enhance the dodecane contact angle values from 69 to 88 degrees owing to the effective surface arrangement ability of the homooligomer on the ***PSt*** particles in the composites. The superhydrophilic characteristic derived from the composites would originate from the presence of hydrophilic DMAA units in cooligomer, and we can observe the flip-flop motion between the oleophobic fluoroalkyl groups and the hydrophilic DMAA units when the environment is changed from air to water to give the oleophobic/superhydrophilic property on the orifice between the ***PSt*** particles as indicated in the following Schematic illustration (see Scheme 2).

In contrast, the presence of the homo- and co-oligomers on the orifice between the ***PSt*** particles cannot be confirmed in the cases of the fluorinated composites possessing higher feed ratios of homooligomer from 72 to 90 mg (Runs 7, 8, and 10 in Figure 3), providing the effective decrease of the dodecane contact angle values from 88 (Run 6) to 68, 35 and 0 degrees (see Table 2). The decrease

of dodecane contact angle values is much related to the decolorization of the red-color (carbon atom) (see Figure 3: Run 7 - (B), Run 8 - (B) and Run 10 - (B)) and the green-color increase (fluorine atom) (see Figure 3: Run 7 - (C), Run 8 - (C) and Run 10 - (C)) on each ***PSt*** particle surface. Thus, higher contents of the homooligomers enable the homooligomer to coat on the ***PSt*** particle surface, compared to the lower contents of the homooligomers, constructing the clear voids moieties between the ***PSt*** particles to supply the superoleophilic/superhydrophilic characteristic due to not only the oleophobic/hydrophobic property related to fluoroalkyl groups but also the hydrophilicity imparted by the DMAA units in cooligomers illustrated in Scheme 3.

On the other hand, Run 11 in Figure 3 indicates the R_F-(VM-$SiO_{3/2}$)$_n$-R_F/***PSt*** composites possessing no fluorinated cooligomer segments can provide a perfect surface arrangement ability of the homooligomer in the composites on the ***PSt*** particles, because we can observe the extremely reduce of the red-color (carbon atom) (Run 11 - (B) in Figure 3) and the effective increase of the green-color (fluorine atom) (Run 11 - (C) in Figure 3). This perfect surface arrangement behavior related to the homooligomer in the composites would be due to the oleophobic/hydrophobic characteristic derived from the homooligomer as indicated in Table 2. Such surface arrangement behavior enables the composites to construct the clear orifice between the ***PSt*** particles, and an oil droplet could easily penetrate into the small orifice between the ***PSt*** particles to provide an

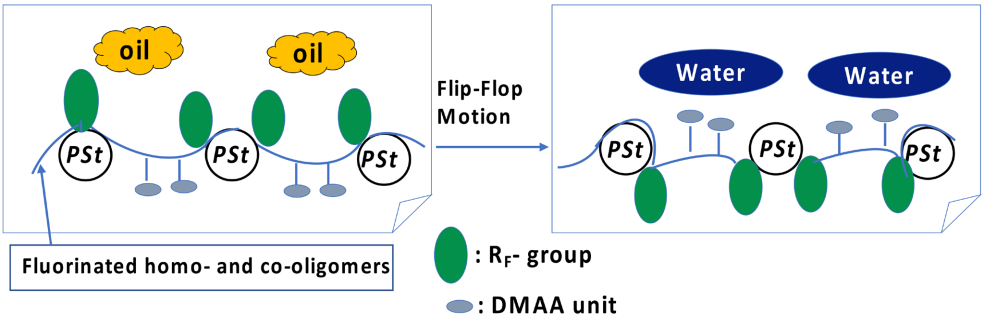

Scheme 2. Schematic illustration for the flip-flop motion between the fluoroalkyl groups and DMAA units in the composites on the orifice between the ***PSt*** particles.

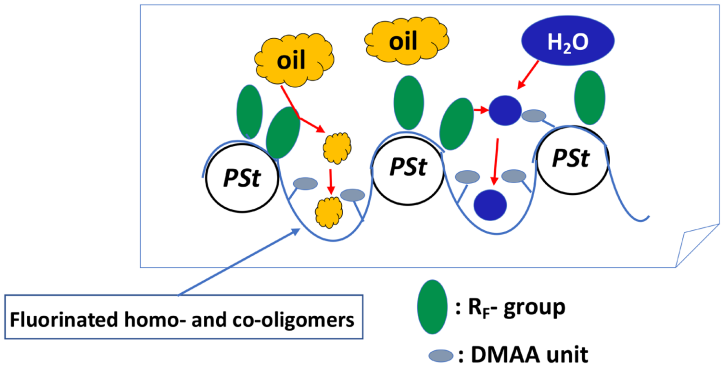

Scheme 3. Schematic illustration for superoleophilic/superhydrophilic behavior on the R_F-(VM-$SiO_{3/2}$)$_n$-R_F/R_F-(VM-$SiO_{3/2}$)$_x$-(DMAA)$_y$-R_F/***PSt*** composites surface.

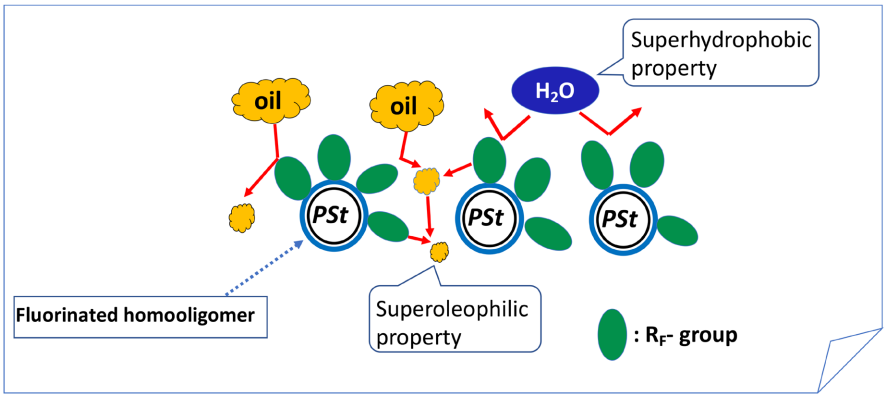

Scheme 4. Schematic illustration for superoleophilic/superhydrophobic behavior on the R_F-(VM-$SiO_{3/2}$)$_n$-R_F/***PSt*** composites surface.

superoleophilic property as illustrated in **Scheme 4**. Since fluorinated homooligomer-coated ***PSt*** particles are micrometer-sized controlled (particle size: 125 m; see Run 11 in **Table 1**), the roughness surface derived from the fluorinated homooligomer/***PSt*** composites can be easily constructed to exhibit a superhydrophobic characteristic on the composite surface (see **Scheme 4**).

It was previously reported that the superhydrophobic surface can be realized by enhancing the surface roughness [20] [21] [22]. Our present fluorinated composites consist of the micrometer-sized controlled particles. Such composite surface would construct the roughness architecture to provide the superhydrophobic characteristic on their surface as illustrated in **Scheme 4**. Superoleophilic surfaces have a strong affinity toward the organic oils. Thus, our present fluorinated composites possessing the superoleophilic/superhydrophobic property will have a wide range of applications such as recovery of oil spilled into seawater [23]-[33]. In addition, the fluorinated composites possessing the highly oleophobic/superhydrophilic property are expected to be applicable to the practical applications such as the water removal from oil [34] [35] [36] [37].

4. Conclusion

Fluoroalkyl end-capped vinyltrimethoxysilane-*N*,*N*-dimethylacrylamide cooligomer [R_F-(VM)$_x$-(DMAA)$_y$-R_F; R_F = $CF(CF_3)OC_3F_7$] was synthesized by the cooligomerization of the corresponding monomers by the use of fluoroalkanoyl peroxide [R_F-C(=O)O-O(O=)C-R_F]. The fluoroalkylated cooligomeric nanoparticles [R_F-(VM-$SiO_{3/2}$)$_x$-(DMAA)$_y$-R_F] prepared by the sol-gel reaction of the cooligomer under alkaline conditions were applied to the surface modification to exhibit the oleophobic/superhydrophilic property on the modified surface; although the fluoroalkyl end-capped vinyltrimethoxysilane homooligomeric nanoparticles [R_F-(VM-$SiO_{3/2}$)$_n$-R_F] prepared under similar sol-gel reactions with the corresponding homooligomer were found to supply the oleophobic/hydrophobic property on the modified surface. R_F-(VM-$SiO_{3/2}$)$_n$-R_F/R_F-(VM-$SiO_{3/2}$)$_x$-(DMAA)$_y$-R_F/***PSt*** composites were prepared by the sol-gel reactions of the homooligomer [R_F-(VM)$_n$-R_F] and the cooligomer [R_F-(VM-SiO)$_x$-(DMAA)$_y$-R_F] in the presence

of the micrometer-sized polystyrene particle (***PSt***) under alkaline conditions. The surface wettability of the obtained composites was studied through the dodecane and water contact angle measurements. Interestingly, we can observe the surface wettability change from the highly oleophobic/superhydrophilic to superoleophilic/superhydrophobic characteristics, increasing with greater feed ratios of the homooligomer in homooligomer/cooligomer employed for the preparation of the composites. Therefore, our present fluorinated composites possessing such unique wettability will have a high potential for a considerable amount of practical applications such as selective water removal from oil and oil removal from industrial wastewater and ocean water. Especially, our present fluorinated oligomeric ***PSt*** composites possessing a superoleophilic/superhydrophobic characteristic will open the new possibility for the capture of the spilled oils on the wastewater and ocean water surface, of whom oil-spillage will be due to the industrial accidents during the oil transport through truck or ship. In addition, the fluorinated ***PSt*** composite particles possessing a superoleophilic/superhydrophobic characteristic should interact effectively with a variety of organic compounds owing to their superoleophilic property, particularly with fluorinated organic molecules through the fluorophilic—fluorophilic interaction between the fluorinated organic molecules and the fluoroalkyl groups in the composite particles. Thus, the present composites will be also expected to apply to the packing material for column chromatography for the efficient separation of the fluorinated organic compounds.

Funding

This work was partially supported by a Grant-in-Aid for Scientific Research 19K05027 from the Ministry of Education, Science, Sports, and Culture in Japan.

Conflicts of Interest

The authors declare no conflicts of interest regarding the publication of this paper.

References

[1] Parida, S.K., Dash, S., Patel, S. and Mishra, B.K. (2006) Adsorption of Organic Molecules on Silica Surface. *Advances in Colloid and Interface Science*, **121**, 77-110. https://doi.org/10.1016/j.cis.2006.05.028

[2] He, H., Gan, Q. and Feng, C. (2017) Preparation and Application of Ni(ii) Ion-Imprinted Silica Gel Polymer for Selective Separation of Ni(ii) from Aqueous Solution. *RSC Advances*, **7**, 15102-15111. https://doi.org/10.1039/C7RA00101K

[3] Tokman, N., Akaman, S. and Ozean, M. (2003) Solid-Phase Extraction of Bismuth, Lead and Nickel from Seawater Using Silica Gel Modified with 3-Aminopropyltriethoxysilane Filled in a Syringe Prior to Their Determination by Graphite Furnace Atomic Absorption Spectrometry. *Talanta*, **59**, 201-205. https://doi.org/10.1016/S0039-9140(02)00479-4

[4] Sui, H., Liu, H., An, P., He, L., Li, X. and Cong, S.J. (2017) Application of Silica Gel in Removing High Concentrations Toluene Vapor by Adsorption and Desorption

Process. *Journal of the Taiwan Institute of Chemical Engineers*, **74**, 218-224. https://doi.org/10.1016/j.jtice.2017.02.019

[5] Vardini, M.T. and Mardani, L. (2018) Surface Imprinting of Silica Gel by Methyldopa and Its Application in the Solid Phase Extraction Produce. *Journal of the Brazilian Chemical Society*, **29**, 310-319.

[6] Guibal, E., Lorenzelli, R., Vincent, T. and Cloirec, P.L. (1995) Application of Silica Gel to Metal Ion Sorption: Static and Dynamic Removal of Uranyl Ions. *Environmental Technology*, **16**, 101-114. https://doi.org/10.1080/09593331608616251

[7] Inukai, Y., Tanaka, Y., Matsuda, T., Mihara, N., Yamada, K., Nambu, N., Itoh, O., Doi, T., Kaida, Y. and Yasuda, S. (2004) Removal of Boron(III) by N-Methylglucamine-Type Cellulose Derivatives with Higher Adsorption Rate. *Analytica Chimica Acta*, **511**, 261-265. https://doi.org/10.1016/j.aca.2004.01.054

[8] Inukai, Y., Kaida, Y. and Yasuda, S. (1997) Selective Adsorbents for Germanium(IV) Derived from Chitosan. *Analytica Chimica Acta*, **343**, 275-279. https://doi.org/10.1016/S0003-2670(97)00009-3

[9] Kim, B.R., Snoeyink, V.L. and Saunders, F.M. (1976) Adsorption of Organic Compounds by Synthetic Resins. *Journal of the Water Pollution Control Federation*, **48**, 120-133. https://doi.org/10.1252/jcej.17.204

[10] Goto, S., Goto, M. and Uchiyama, S. (1984) Adsorption Equilibria of Phenol on Anion Exchange Resins in Aqueous Solution. *Journal of Chemical Engineering of Japan*, **17**, 204-205.

[11] Parrino, F. and Palmisano, L. (Eds.) (2021) Titanium Dioxide TiO_2 and Its Applications. Elsevier, Amsterdam.

[12] Wang, Y., Li, J., Wang, L., Xue, T. and Qi, T. (2010) Preparation of Rutile Titanium Dioxide White Pigment via Doping and Calcination of Metatitanic Acid Obtained by the NaOH Molten Salt Method. *Industrial & Engineering Chemistry Research*, **49**, 7693-7696. https://doi.org/10.1021/ie1007147

[13] Tian, C., Huang, S. and Yang, Y. (2013) Anatase TiO_2 White Pigment Production from Unenriched Industrial Titanyl Sulfate Solution via Short Sulfate Process. *Dyes and Pigments*, **96**, 609-613. https://doi.org/10.1016/j.dyepig.2012.09.016

[14] Li, J., Wan, H., Ye, Y., Zhou, H. and Chen, J. (2012) One-Step Process to Fabrication of Transparent Superhydrophobic SiO_2 Paper. *Applied Surface Science*, **261**, 470-472. https://doi.org/10.1016/j.apsusc.2012.08.034

[15] Zhang, M., Wang, C., Wang, S., Shi, Y. and Li, J. (2012) Fabrication of Coral-Like Superhydrophobic Coating on Filter Paper for Water-Oil Separation. *Applied Surface Science*, **261**, 764-769. https://doi.org/10.1016/j.apsusc.2012.08.097

[16] Suzuki, J., Takegahara, Y., Oikawa, Y., Aomi, Y. and Sawada, H. (2018) Preparation of Fluoroalkyl End-Capped Oligomer/Cyclodextrin Polymer Composites: Development of Fluorinated Composite Material Having a Higher Adsorption Ability toward Organic Molecules. *Journal of Encapsulation and Adsorption Sciences*, **8**, 117-138. https://doi.org/10.4236/jeas.2018.82006

[17] Sawada, H., Chiba, M., Honma, G., Yamashita, K. and Suzuki, J. (2020) Preparation of Fluoroalkyl End-Capped Vinyltrimethoxysilane Oligomer/Micro-Sized Silica Composites Possessing Superoleophilic/Superhydrophobic Characteristic: Application to Selective Removal of Aromatic Compounds from Aqueous Methanol Solution by Using These Composites. *Journal of Sol-Gel Science and Technology*, **96**, 636-648. https://doi.org/10.1007/s10971-020-05351-7

[18] Sawada, H., Ikematsu, Y., Kawase, T. and Hayakawa, Y. (1996) Synthesis and Surface Properties of Novel Fluoroalkylated Flip-Flop-Type Silane Coupling Agents. *Lang-*

muir, **12**, 3529-3530. https://doi.org/10.1021/la951041p

[19] Sawada, H. and Nakayama, M.J. (1991) Synthesis of Fluorine-Containing Organosilicon Oligomers. *Journal of the Chemical Society, Chemical Communications*, 677-678. https://doi.org/10.1039/c39910000677

[20] Kota, A.K., Li, Y., Marby, J.M. and Tuteja, A. (2012) Hierarchically Structured Superoleophobic Surfaces with Ultralow Contact Angle Hysteresis. *Advanced Materials*, **24**, 5838-5843. https://doi.org/10.1002/adma.201202554

[21] Deng, X., Mammen, L., Butt, H.-J. and Vollmer, D. (2012) Candle Soot as a Template for a Transparent Robust Superamphiphobic Coating. *Science*, **335**, 67-70. https://doi.org/10.1126/science.1207115

[22] Yao, X., Song, Y. and Jiang, L. (2011) Applications of Bio-Inspired Special Wettable Surfaces. *Advanced Materials*, **23**, 719-734. https://doi.org/10.1002/adma.201002689

[23] Zhang, D., Liu, F., Zhang, M., Gao, Z. and Wang, C. (2015) Novel Superhydrophobic and Superoleophilic Sawdust as a Selective Oil Sorbent for Oil Spill Cleanup. *Chemical Engineering Research and Design*, **102**, 35-41. https://doi.org/10.1016/j.cherd.2015.06.014

[24] Zhang, M., Wang, C., Wang, S., Shi, Y. and Li, J. (2013) Fabrication of Superhydrophobic Cotton Textiles for Water-Oil Separation Based on Drop-Coating Route. *Carbohydrate Polymers*, **97**, 59-64. https://doi.org/10.1016/j.carbpol.2012.08.118

[25] Arbatan, T., Zhang, L., Fang, X.-Y. and Shen, W. (2012) Cellulose Nanofibers as Binder for Fabrication of Superhydrophobic Paper. *Chemical Engineering Journal*, **210**, 74-79. https://doi.org/10.1016/j.cej.2012.08.074

[26] Si, Y. and Guo, Z. (2015) Superwetting Materials of Oil-Water Emulsion Separation. *Chemistry Letters*, **44**, 874-883. https://doi.org/10.1246/cl.150223

[27] Liu, K., Tian, Y. and Jiang, L. (2013) Bio-Inspired Superoleophobic and Smart Materials: Design, Fabrication, and Application. *Progress in Materials Science*, **58**, 503-564. https://doi.org/10.1016/j.pmatsci.2012.11.001

[28] Darmanin, T. and Guittard, F. (2014) Wettability of Conducting Polymers: From Superhydrophilicity to Superoleophobicity. *Progress in Polymer Science*, **39**, 656-682. https://doi.org/10.1016/j.progpolymsci.2013.10.003

[29] El-Gawad, H.S.A. (2014) Oil and Grease Removal from Industrial Wastewater Using New Utility Approach. *Advances in Environmental Chemistry*, **2014**, Article ID: 916878. https://doi.org/10.1155/2014/916878

[30] da Costa Cunha, G., Pinho, N.C., I.Silva, A.A., Siva, L.S., Costa, J.A.S., da Silva, C.M.P., Romao, L.P.C. (2019) Removal of Heavy Crude Oil from Water Surfaces Using a Magnetic Inorganic-Organic Hybrid Powder and Membrane System. *Journal of Environmental Management*, **247**, 9-18. https://doi.org/10.1016/j.jenvman.2019.06.050

[31] Gkogkou, D., Rizogianni, S., Tziasiou, C., Gouma, V., Pourna, A.D., Giokas, D.L., Manos, M.J. (2021) Highly Efficient Removal of Crude Oil and Dissolved Hydrocarbons from Water Using Superhydrophobic Cotton Filters. *Journal of Environmental Chemical Engineering*, **9**, Article ID: 106170. https://doi.org/10.1016/j.jece.2021.106170

[32] Wang, J., Zhang, X., Lu, H., Fu, Y., Xu, M., Jiang, X. and Wu, J. (2021) Superhydrophobic Nylon Fabric with Kaolin Coating for Oil Removal under Harsh Water Environments. *Applied Clay Science*, **214**, Article ID: 106294. https://doi.org/10.1016/j.clay.2021.106294

[33] Wang, Y., Yan, J., Wang, J., Zhang, X., Wei, L., Du, Y., Yu, B. and Ye, S. (2020) Superhydrophobic Metal Organic Framework Doped Polycarbonate Porous Monolith for Efficient Selective Removal Oil from Water. *Chemosphere*, **260**, Article ID: 127583.

https://doi.org/10.1016/j.chemosphere.2020.127583

[34] Wu, J., Yin, K., Li, M., Xiao, S., Wu, Z., Wang, K., Duan, J.-A. and He, J. (2020) Femtosecond Laser Manipulating Underoil Surface Wettability for Water Removal from Oil. *Colloid Surfaces A*, **601**, Article ID: 125030. https://doi.org/10.1016/j.colsurfa.2020.125030

[35] Tsai, Y.-T., Maggay, I.V., Venault, A. and Lin, Y.-F. (2021) Fluorine-Free and Hydrophobic/Oleophilic PMMA/PDMS Electrospun Nanofibrous Membranes for Gravity-Driven Removal of Water from Oil-Rich Emulsions. *Separation and Purification Technology*, **279**, Article ID: 119720. https://doi.org/10.1016/j.seppur.2021.119720

[36] Molla, S.H., Masliyah, J.H. and Bhattacharjee, S. (2005) Simulations of a Dielectrophoretic Membrane Filtration Process for Removal of Water Droplets from Water-in-Oil Emulsions. *Journal of Colloid and Interface Science*, **287**, 338-350. https://doi.org/10.1016/j.jcis.2004.06.096

[37] Petchsoongsakul, N., Ngaosuwan, K., Kiatkittipong, W., Wongsawaeng, D. and Assabumrungrat, S. (2020) Different Water Removal Methods for Facilitating Biodiesel Production from Low-Cost Waste Cooking Oil Containing High Water Content in Hybridized Reactive Distillation. *Renewable Energy*, **162**, 1906-1918. https://doi.org/10.1016/j.renene.2020.09.115